



Contents lists available at ScienceDirect

## Asian Pacific Journal of Tropical Disease

journal homepage: www.elsevier.com/locate/apjtd



Floral research

doi: 10.1016/S2222-1808(16)61085-X

©2016 by the Asian Pacific Journal of Tropical Disease. All rights reserved.

Biological application of green silver nanoparticle synthesized from leaf extract of *Rauvolfia serpentina* Benth

Sudipta Panja, Indranil Chaudhuri, Kalyani Khanra, Nandan Bhattacharyya\*

Department of Biotechnology, Panskura Banamali College, Panskura RS, PIN-721152, Purba Medinipur, West Bengal, India

## ARTICLE INFO

## Article history:

Received 4 Apr 2016

Received in revised form 12 May, 2nd

revised form 18 May 2016

Accepted 10 Jun 2016

Available online 23 Jun 2016

## Keywords:

Antimicrobial activity

Cytotoxicity

Larvicidal activity

*Rauvolfia serpentina* Benth

Silver nanoparticle

Transmission electron microscopy

X-ray diffraction

## ABSTRACT

**Objective:** To synthesize silver nanoparticles (AgNPs) from the leaf extract of *Rauvolfia serpentina* Benth and examination of their various biological activities.**Methods:** An ecofriendly, easy, one step, non-toxic and inexpensive approach is used, where aqueous plant extract acts as a reducing as well as stabilizing agent of AgNPs. The nanoparticles were characterized by UV-vis spectroscopy, Fourier transform infrared spectroscopy, transmission electron microscopy, X-ray diffraction, and energy-dispersive X-ray spectroscopy analysis.**Results:** Surface plasmon resonance of the nanoparticles was observed at 427 nm in UV-vis spectroscopy. Fourier transform infrared spectroscopy result confirms that the plant extract acts as the reducing as well as the capping agent of the AgNPs. Transmission electron microscopy indicated that the synthesized nanoparticles are spherical in shape and approximately 7–10 nm in size, whereas the crystalline nature with face-centered cubic structure of the AgNPs was detected by X-ray diffraction analysis. Presence of silver in the AgNPs is 31.43% by weight, as confirmed by energy-dispersive X-ray spectroscopy. The synthesized AgNPs have antimicrobial activities against human pathogenic microorganisms. It also shows larvicidal activity and cytotoxicity against HeLa, MCF-7 cell lines.**Conclusions:** Synthesized spherical shaped AgNPs from the leaf extract of *Rauvolfia serpentina* Benth have antimicrobial and larvicidal activities as well as cytotoxicity against HeLa and MCF-7 cell lines.

## 1. Introduction

Nanoparticle is defined as a cluster of atoms between 1 to 100 nm in size, behaving like a whole unit in respect of all its properties[1]. The demand of nanoparticle in different field is increased day by day due to its large surface to volume ratio, optical property, quantum confinement in semiconductor particles, surface plasmon resonance (SPR) in some metal particles and superparamagnetism in magnetic materials, electronic, biological labeling[2], photo-electrochemical and antibacterial properties. The interaction between the surfaces of the nanoparticle and the solvent is strong enough to overcome density differences, resulting in the suspension of nanoparticles. Nanoparticles have high driving force for diffusion due to its high surface area to volume ratio and have both hydrophilic and hydrophobic regions due to which it can self-assemble as water/oil interfaces and act as solid surfactants.

Nanoparticles are synthesized, having either top-down or bottom-up approaches. The basis of top-down approach is mechanical breakdown of bulk materials to nanoscale structure. The bottom-up approach is based on the assembly of atoms or molecules to form a nanoscale structure. Both the chemical and biological nanoparticle synthesis contain bottom-up approach[3]. The well-defined chemical and physical methods for nanoparticle synthesis are expensive and involve the use of toxic chemical which may be absorbed on the surface of the nanoparticle. In some biomedical application, the nanoparticles have direct contact with the human body, which is harmful for the body. The biologically synthesized nanoparticles may be less toxic. Biologically synthesized nanoparticles are formed by the ionic or electronic interaction between the metal complex and the functional group is present in the biomass. There are many bioorganic compounds like flavonoids, terpenoids, proteins, reducing sugars and alkaloids involved in either reducing or capping agents during the formation of nanoparticles[4]. Reducing agent, stabilizing agent and a solvent to solubilize the concerned metal are mainly required for the synthesis of nanoparticle. The plant biomass acts as both reducing agent and stabilizing agent and the solvent is an aqueous solution which is cost effective and ecofriendly. There are many examples of green synthesis of silver nanoparticle (AgNP) by using plant extract as reducing or capping agents such as

\*Corresponding author: Prof. Dr. Nandan Bhattacharyya, Department of Biotechnology, Panskura Banamali College, Panskura RS, PIN-721152, Purba Medinipur, West Bengal, India.

Tel: +91 9434453188

E-mail: bhattacharyya\_nandan@rediffmail.com

The journal implements double-blind peer review practiced by specially invited international editorial board members.

*Argemone mexicana* leaf extract[5], *Mikania cordata* leaf extract[6], *Pterocarpus santalinus* leaf extract[7]. The properties of nanoparticles depend on their size, shape, and crystal structure[8]. The shape of the nanoparticle depends on the concentration of bioorganic compounds. Silver and gold are widely used in the synthesis of nanoparticle due to its large positive electrochemical potential.

AgNPs acts as biological labeling agents, drug carriers and imaging agent. AgNPs are used in drug delivery, food industries, agriculture, textile industries, and cosmetics as antioxidant, antimicrobial, anti-cancer and larvicides[7].

*Rauvolfia serpentina* Benth. (*R. serpentina*) (Figure 1) is commonly known as 'sarpagandha' or snakeroot. It belongs to the Apocynaceae family. It is an important Ayurvedic shrub about 30 to 90 cm in height with white and pinkish flower. The plant is available in tropical regions of the Indian subcontinent and East Asia. *R. serpentina* contains many bioactive chemicals such as reserpine, ajmaline, yohimbine, serpentinine, deserpidine, rescinnamine, etc. The root and leaf extracts of *R. serpentina* have a good medicinal value and are traditionally used as medicine in India. It is used for the treatment of various central nervous system disorders[9], high blood pressure[10], lack of sleeping, nervousness, hypertension[11], and various mental disorders. It resists prostate cancer, too[12]. It is also used for snake bite. It is the most important plant used in traditional Chinese medicine.



Figure 1. Whole plant of *R. serpentina*.

Nowadays many human pathogens are resistant to common drugs which have become threat to human civilization. Considering the above points, our main objectives are to synthesize and characterize AgNP from the leaf extract of *R. serpentina* as well as to study the antimicrobial, antifungal, larvicidal activities of the synthesized AgNP and to study the cytotoxicity of the AgNP against two different cancer cell lines.

## 2. Materials and methods

### 2.1. Agents

Luria-Bertani medium, silver nitrate, and MTT were purchased from Himedia (Bangalore, India). All the chemicals are analytical grades. Deionized water was obtained from National Chemical Co., Kolkata, India. For antimicrobial activity study *Bacillus subtilis* (*B. subtilis*), *Pseudomonas aeruginosa* (*P. aeruginosa*), *Enterococcus faecalis* (*E. faecalis*), *Escherichia coli* (*E. coli*), *Aspergillus niger* (*A. niger*) and *Candida albicans* (*C. albicans*) were collected from

the Microbial Type Culture Collection and Gene Bank, Chandigarh, India. These strains were cultured and maintained according to their specifications.

### 2.2. Collection of plant materials and preparation of plant aqueous extract

The plant, *R. serpentina* was collected in the middle of April, 2015 in the afternoon from Amlachati, Jhargram, Paschim Medinipur, West Bengal, India (22°22'36" N, 87°02'36" E). The plant was identified and authenticated by the experts of *Ex-situ* Propagation Centers, Amlachati and a scientist of Botany Department of our college. The voucher specimen was submitted to our college collections. At first 10 g of plant samples were washed with distilled water and dried with tissue paper. Then the leaves were cut into small pieces and homogenized with 100 mL sterilized distilled water. After that it was boiled for 1 h at 80 °C in a water bath and the extract was filtered through 0.6 µm sized filters.

### 2.3. Synthesis of AgNP

For the synthesis of AgNPs, 10 mmol/L silver nitrate stock solution was prepared in deionized water. AgNPs were synthesized by varying conditions of the reactions. In the first set of reactions, the concentration of silver nitrate was kept constantly at 1 mmol/L, plant extract volume was varied from 1 mL to 5 mL in total 10 mL of reaction mixtures. In another set 1 mL of plant extract was added to different concentrations of silver nitrate (1 to 5 mmol/L) keeping the reaction volume same as before[13]. To study the effect of temperature and incubation time on the synthesis of AgNPs, silver nitrate concentration and plant extract volume were kept at 1 mmol/L, 1 mL respectively in different sets of reactions. Color change of the solution from pale to dark brown indicated the synthesis of AgNPs (Figure 2)[14]. The solution contains AgNPs as well as many impurities[15,16]. The colloidal solution was subjected to centrifugation at 8000 r/min for 30 min[17]. The pellet was re-suspended in sterile distilled water and centrifuged at the same condition for 3 to 4 times for washing. Finally, the pellet was air dried.

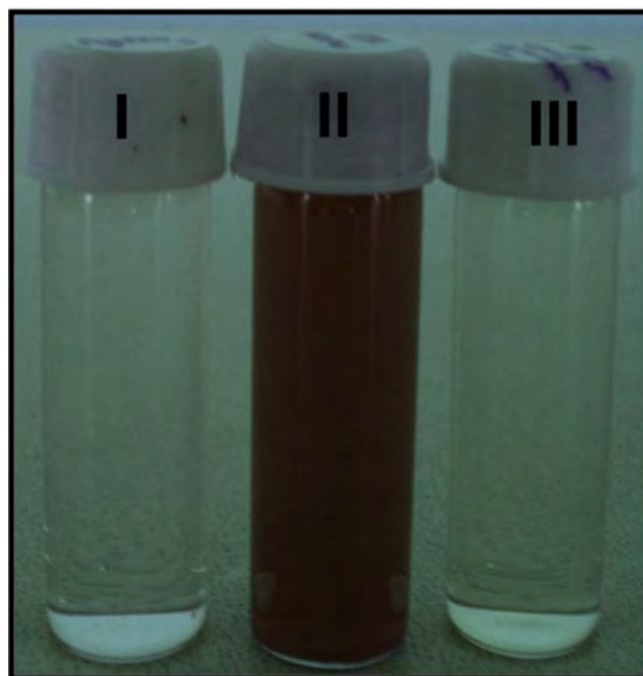


Figure 2. Color changes during nanoparticle synthesis.

I: Leaf extract of *R. serpentina*; II: Silver nanoparticle synthesized from leaf extract of *R. serpentina*; III: 1 mmol/L silver nitrate solution.

## 2.4. Characterization of AgNP

### 2.4.1. UV-vis spectroscopy

During the AgNPs synthesis in aqueous solution, the reduction of  $\text{Ag}^+$  to  $\text{Ag}^0$  and the formation of colloidal silver with particle diameter of several nanometers take place. Colloidal particles which are smaller than visible wavelengths show a band in the UV-vis range. This happens due to the collective oscillation of the electron. This phenomenon is known as SPR which is the signature of AgNP. As the particle size increases the band shifts to the longer wavelength. Longer tailing in the band indicates agglomeration of AgNPs resulting in large size of particle. UV-vis spectral analysis was done by using spectrophotometer (Biospectrometer, Eppendorf) and by scanning the spectra between 300–800 nm at the resolution of 1 nm[18].

### 2.4.2. Transmission electron microscopy (TEM)

TEM is used to study the size and shape of the nanoparticles. In this study the aqueous solution of nanoparticle was dropped on carbon coated copper grids and was allowed to evaporate. The extra solution was removed by using tissue paper. A beam of electrons is transmitted through an ultra-thin specimen. The image was magnified and focused onto an imaging device. A JEM-1200EX electron microscope (JEOL, Tokyo, Japan) was used in this study with 120 kV accelerating voltage. Diameters of more than 135 particles were measured to obtain the size distribution of the synthesized AgNPs with the help of origin 7.5 software (Origen Lab Corporation, Northampton, Massachusetts, USA), and were confirmed by making the calculations with the use of Debye-Scherrer equation ( $D = K\lambda/\beta\cos\theta$ ) from the highest intensity of XRD pattern. The chemical characterization of the synthesized AgNP was performed by using energy-dispersive X-ray spectroscopy (EDX) analysis. The AgNPs were dehydrated and drop coated on to carbon film.

### 2.4.3. X-ray diffraction (XRD) measurements

XRD is used to know the face center cubic crystalline nature of the synthesized nanoparticles. The dried AgNPs powder is coated on XRD copper grid. The XRD is measured by a X'PERT-PRO X-ray diffractometer, operated at a voltage of 40 kV and a current of 30 mA. The spectrum is recorded using Cu K $\alpha$  radiation in the range of  $2\theta$  from  $20^\circ$  to  $100^\circ$ . The average crystallite domain size is calculated from the width of the XRD peaks, using the Scherrer's formula  $D = 0.94\lambda/\beta \cos\theta$  (where  $\lambda$  is the X-ray wavelength, D is the average crystallite domain size perpendicular to the reflecting planes,  $\beta$  is the full width at half maximum, and  $\theta$  is the diffraction angle)[6,7,18].

### 2.4.4. Fourier transform infrared spectroscopy (FTIR) measurements

Dried AgNPs are mixed with KBr salt (1:99) and then are compressed to prepare a salt disc. Then the FTIR spectra is recorded using a Perkin-Elmer spectrometer FTIR Spectrum Two in the range  $4000\text{--}400\text{ cm}^{-1}$  at a resolution of  $4\text{ cm}^{-1}$ .

## 2.5. Biological application

### 2.5.1. Study of the antibacterial activity of the AgNP

The antibacterial activity of the biosynthesized AgNPs from *R. serpentina* is carried out against human pathogenic Gram-positive bacteria, *B. subtilis*, *E. faecalis* and Gram-negative bacteria, *P. aeruginosa*, *E. coli*. Antimicrobial activity is studied by well diffusion method using four various concentrations (25  $\mu\text{g/mL}$ , 50  $\mu\text{g/mL}$ , 75  $\mu\text{g/mL}$  and 150  $\mu\text{g/mL}$ ) of AgNPs, using ciprofloxacin as standard antibiotic at the same concentrations[16,19-22]. A total of 200  $\mu\text{L}$  of overnight grown cultures of each bacterial strains ( $1 \times 10^5$  CFU/mL) in Luria-Bertani are used to prepare bacterial lawns on the agar plates and incubated over night at  $37^\circ\text{C}$ . The wells, prepared with

the help of a sterilized stainless steel cork borer, are loaded with 50  $\mu\text{L}$  of different concentration of synthesized AgNP and ciprofloxacin as positive control. The plates are incubated at  $37^\circ\text{C}$  for 18 h. The zone of inhibitions (ZOI) is measured by using antibiotic zonescale (Himedia, India). The mean value of the triplicate of the experiment is expressed in millimeter unit.

### 2.5.2. Determination of fungicidal activity of the synthesized AgNP

The fungicidal activity of the synthesized AgNP is studied against two human pathogenic fungi *A. niger* and *C. albicans* by using agar well diffusion method[23-25]. The fungal strains are maintained in potato dextrose agar. A mat is prepared on potato dextrose agar plate by using 200  $\mu\text{L}$  of 72 h grown fungal cultures. The wells on the potato dextrose agar plate are created by using a 6-mm sterile stainless steel cork borer and loaded with 50  $\mu\text{L}$  of different concentrations (25  $\mu\text{g/mL}$  to 150  $\mu\text{g/mL}$ ) of AgNPs in each well. The plates are incubated at room temperature for 72 h, and the ZOI is measured by using an antibiotic zonescale (Himedia, India). The mean value of the triplicate of the experiment is expressed in millimeter unit.

### 2.5.3. Study the larvicidal activity of the synthesized AgNP

The larvicidal activity of the synthesized AgNP is tested against third instar mosquito larvae of *Culex quinquefasciatus* (*Cx. quinquefasciatus*). The test is performed in Petri plate, using four different concentrations (2.5  $\mu\text{g/mL}$ , 5  $\mu\text{g/mL}$ , 10  $\mu\text{g/mL}$  and 25  $\mu\text{g/mL}$ ) of synthesized AgNPs[26,27]. Seven Petri plates are taken. A total of 20 mL of each four different above-mentioned concentration of AgNPs are taken into four different Petri plates. One of them contains only 20 mL of triple distilled water as control, one contains 20 mL 1 mmol/L silver nitrate solution and the other contains only 20 mL of the plant extract. Ten healthy freshly washed larvae are kept into each plate at room temperature. After 12 h, the result is recorded. The total process is repeated three times. The percent of mortality is calculated by using the following formula[28],  

$$\% \text{ Mortality} = [(\% \text{ test mortality} - \% \text{ control mortality}) / (100 - \% \text{ control mortality})] \times 100$$

### 2.5.4. Cytotoxicity study of the AgNP

MTT assay are used to determine the cell viability and cytotoxicity. The basic principle of MTT assay is mitochondria of viable cell release dehydrogenases which reduced MTT to water insoluble blue formazan crystal. This crystal is soluble in dimethyl sulfoxide. The difference between colour development between viable and nonviable cells is measured by an ELISA redder (Robonik, Readwell touch ELISA plate analyzer, India). In this study HeLa (human cervical cancer cell line) and MCF-7 (human breast cancer cell line) cells are seeded in a 96-well tissue culture plate. After 24 h the cells are treated with five different doses (1  $\mu\text{g/mL}$ , 2.5  $\mu\text{g/mL}$ , 5  $\mu\text{g/mL}$ , 10  $\mu\text{g/mL}$ , 25  $\mu\text{g/mL}$ ) of synthesized AgNP. Non-treated cells are used as control. Overnight incubated cultured cells are then subjected to 0.5 mg/mL concentration of MTT. Then the cells are incubated at  $37^\circ\text{C}$  for 3.5 h. After that, the formazon is dissolved by adding 100  $\mu\text{L}$  of dimethyl sulfoxide into each well of the 96 well tissue culture plates. After 10 min of low speed shaking the colour changes are recorded[6,29,30]. The rate of survival of the treated cells is determined as follows:

$$\text{Cell viability (\%)} = (1 - \text{OD At}/\text{OD Ac}) / 100$$

Where Ac is absorbency of control cells and At is absorbency of treated cells.

## 2.6. Statistical analysis

In present study all the experiments are carried out in triplicate.

The obtained data are expressed and analyzed in mean  $\pm$  SD. The graphs display error bars for the selected chart series with 5% value.

### 3. Results

#### 3.1. UV-vis spectroscopy analysis

UV-vis spectroscopy analysis is the signature of AgNP synthesis from plant extract in presence of silver nitrate solution. Various reports show that the color changes from light yellow to brown (Figure 2) and resonance peak of AgNP appearing in the region 412 nm to 453 nm [7,18,31-33] is the signature of AgNP formation. The color changes during the formation of AgNP due to the excitation of surface plasmon vibrations. The peak in the visible region indicates the reduction of the  $\text{Ag}^+$  and the synthesis of AgNP from leaf extract of *R. serpentina*. To study the effect of incubation time on AgNP synthesis, each of seven tubes contains 9 mL of 1 mmol/L silver nitrate solution and 1 mL of leaf extract are added and incubated at 90 °C for different times (the meaning would be clearer if these long sentences are broken into shorter ones). Initially, no peak is observed. With time, the intensity increases. Up to 45 min of incubation the tail of the peak becomes long, indicating the aggregation of the particle. After 60 min, it is observed that the SPR band appears at 427 nm with a sharp band. Then, with the increase of the incubation time, a broad SPR band is observed with longer tailing. It indicates that the size of the synthesized nanoparticle increases (Figure 3A). To study the effect of temperature on the synthesis of AgNPs, 9 mL of 1 mmol/L silver nitrate solution and 1 mL of leaf extract are incubated for 60 min at different temperatures. No significant SPR band is observed up to incubation temperature 50 °C. At incubation temperature 70 °C a broad SPR band is observed with long tailing. At incubation temperature 90 °C, a sharp SPR band is observed at 427 nm (Figure 3B). To understand the effect of silver nitrate concentration on the formation of AgNPs, five

different concentrations of silver nitrate solution (1, 2, 3, 4, 5 mmol/L) are taken. It is observed that with the increase of the concentration of silver nitrate solution the intensity enhanced and gives an increasingly sharp SPR band around 427 nm. When the concentration of silver nitrate is lower than 4 mmol/L there are SPR bands with long tailing which indicate the aggregation of AgNPs (Figure 3C). Different volumes of the leaf extract (1, 2, 3, 4, 5 mL) are added to 1 mmol/L silver nitrate solution keeping 10 mL volume fixed. With increasing volume of plant extract up to 4 mL the intensity increases, and at volume of 5 mL it decreases. At plant extract volume 4 mL, a sharp SPR band is observed at 427 nm. Below and above plant extract concentration 4 mL the SPR band shows longer tailing and higher wavelengths which indicate the formation of large-sized AgNP (Figure 3D). When AgNP is synthesized from 4 mL leaf extract of *R. serpentina* and 4 mmol/L silver nitrate solution by keeping total volume 10 mL and is incubated at 90 °C for 60 min, a sharp SPR peak is observed at 427 nm (Figure 4).

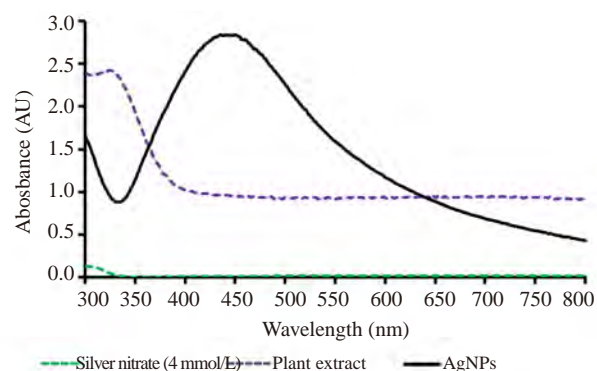


**Figure 4.** UV-vis spectra showing absorbance with 4 mL of leaf extract of *R. serpentina* and 4 mmol/L silver nitrate solution by keeping total volume 10 mL and was incubated at 90 °C for 60 min.

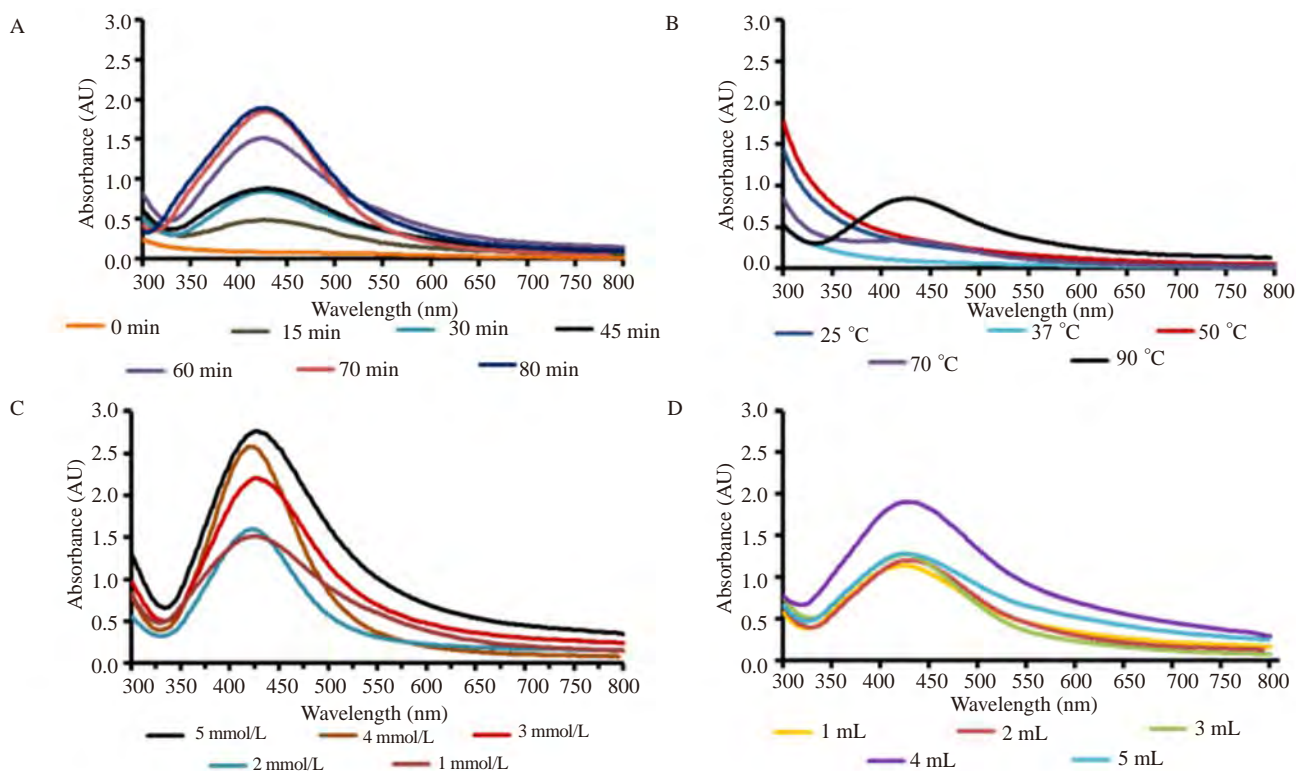


**Figure 3.** UV-vis spectra showing absorbance at different time interval (A), different temperature (B), (C) different concentration of silver nitrate, (D) different concentrations of leaf extract.

### 3.2. TEM analysis

Transmission electron microscopy is used to study the shape and size of the biosynthesized AgNP. By analyzing the images of high resolution TEM image (Figure 5A–D), it is confirmed that the shape of the nanoparticle is likely to be spherical. The average diameter of the biosynthesized AgNPs is between 7 and 10 nm. The internal spacing between the two planes is approximately 0.205 nm and there are approximately 36 planes present in a biosynthesized AgNPs (Figure 5C). Small percentage of synthesized AgNPs is partially aggregated, but is uniform in size and shape with the non-aggregated ones. The (Figure 5D) represents selected area electron diffraction pattern of the synthesized AgNPs. The polycrystalline diffraction rings of synthesized AgNPs can be indexed at (111), (200), (220) and (311). The interplanar spacing which is observed in the Figure 5D, refers to the face centered cubic crystalline structure and high crystalline nature of the biosynthesized AgNP from the leaf extract of *R. serpentina*.

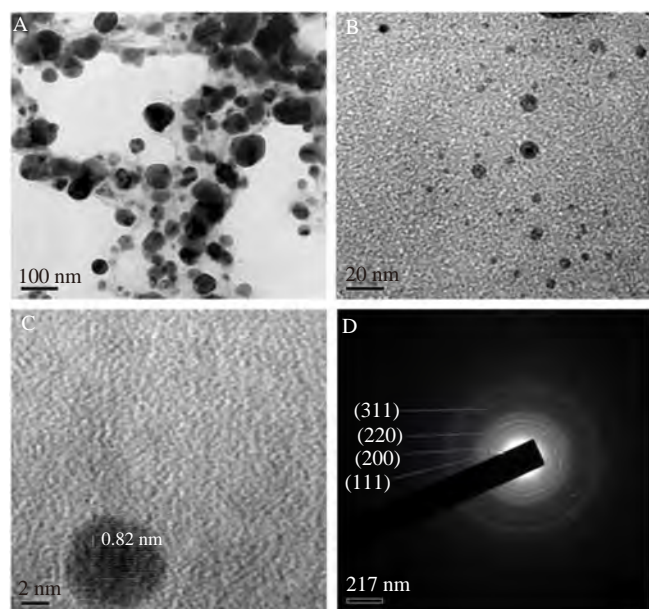


**Figure 5.** TEM images of the synthesized AgNP in three magnifications (A) 100 nm (B) 20 nm (C) 2 nm and (D) selected area electron diffraction pattern.

### 3.3. EDX analysis

EDX spectrum analysis is done to know the elementary composition of the biosynthesized AgNP. The EDX spectrum (Figure 6) of the AgNP shows a distinct signal at 3 KeV region indicating the formation of AgNP from the leaf extract of *Rauvolfia serpentina*[34]. The spectrum also indicates that the peaks are formed as a result of the existence of copper and carbon which might be coming from the carbon coated copper grids. The EDX data shows that the biosynthesized AgNPs contain 31.43% silver by weight.

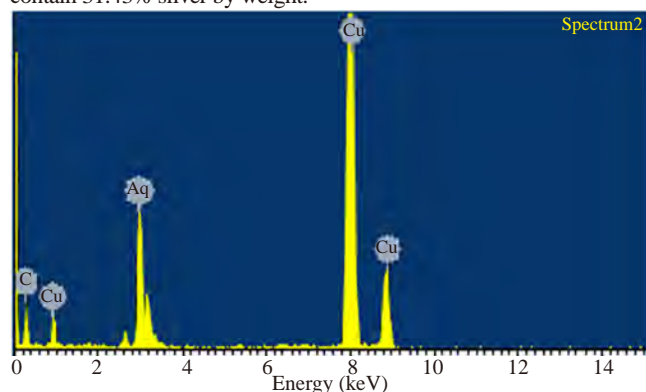


**Figure 6.** EDX spectrum analysis of the synthesized AgNPs.

### 3.4. XRD analysis

The crystalline nature of the synthesized AgNP is confirmed by XRD. Three major peaks are observed in the XRD spectrum. XRD spectrum shows separate peaks at  $2\theta = 38.23^\circ$ ,  $44.42^\circ$ ,  $64.44^\circ$ , and  $77.39^\circ$ , which correspond to (111), (200), (220) and (311), respectively. The XRD spectrum of AgNP synthesized from the leaf extract of *R. serpentina* is analyzed in respect of standard AgNP published in Joint Committee on Powder Diffraction Standards (JCPDS file No. 04-0783) (Figure 7). Same type of XRD peaks of AgNP synthesized from plant extract are also reported by Kathiraven *et al.* and Paul *et al.*[35,36]. The broad bottom and sharp peak indirectly indicate the smaller size and crystalline nature of the synthesized nanoparticle.

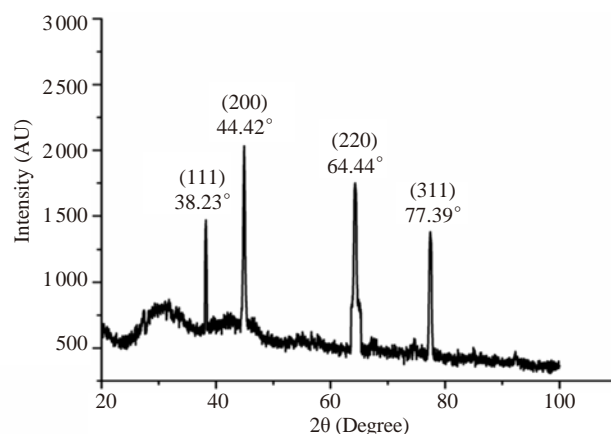


**Figure 7.** XRD pattern of the synthesized AgNPs.

### 3.5. FTIR analysis

FTIR analysis is used to confirm the dual role of the plant extract as a reducing agent for the reduction of the  $\text{Ag}^+$  ions and capping of the reduced AgNPs synthesized from the leaf extract of *R. serpentina*. FTIR analysis also confirms the presence of a functional group in the synthesized AgNPs[7,37]. FTIR spectrum of AgNPs shows major peaks at the position of  $3462$ ,  $1584$ ,  $1381$ ,  $1264$ ,  $1093$  and  $805 \text{ cm}^{-1}$  (Figure 8). A broad signal at  $3462 \text{ cm}^{-1}$  represents the N-H stretching vibration of  $\text{NH}_2$  group[13]. This band may also indicate the O-H stretch or H-bond present in phenol, polyphenol, protein or polysaccharides. A band at  $2971 \text{ cm}^{-1}$  represents the aliphatic C-H stretching vibrations. The peak at  $1637 \text{ cm}^{-1}$  corresponds to  $(\text{NH})=\text{O}$  stretching[35]. Bands at  $1584 \text{ cm}^{-1}$  can confirm the presence of  $=\text{C}=\text{C}=\text{stretch}$  in alkenes. The signal at  $1381 \text{ cm}^{-1}$  indicates C-O-stretching modes and bands at  $1093 \text{ cm}^{-1}$  for C-O-C stretching modes of flavonoids and terpenoids[7,13]. The sharp intense band observed at  $1264 \text{ cm}^{-1}$  and  $805 \text{ cm}^{-1}$  confirms the presence of alkyl halides. The components of plant extract such as tannins, phenols, terpenoids, flavonoids and amide groups of protein are primarily responsible for the reduction as well as capping during the synthesis of AgNPs.

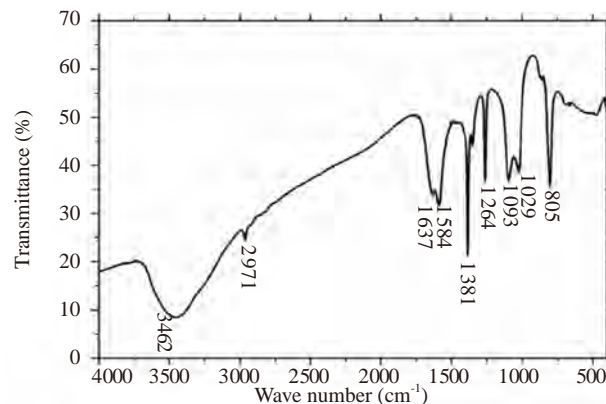


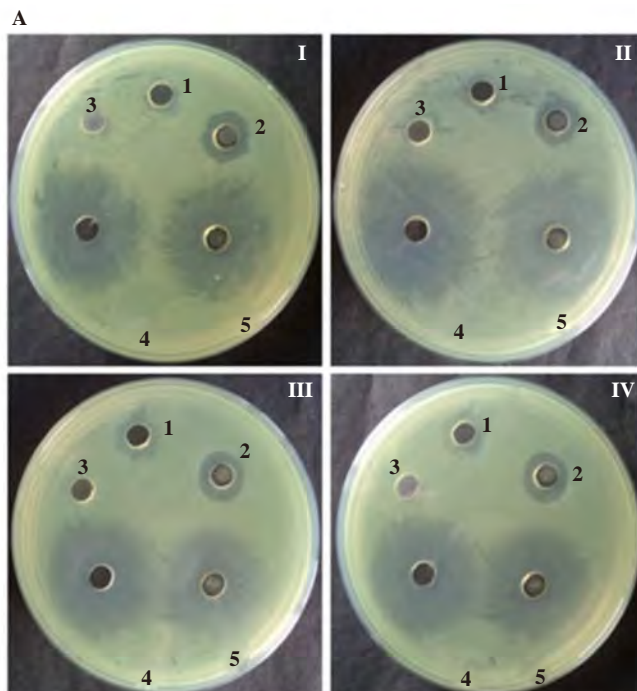
**Figure 8.** FTIR spectra of the synthesized AgNPs.

### 3.6. Antibacterial activity of the AgNP

After 18 h of incubation, the synthesized AgNPs show ZOI against both Gram-positive and Gram-negative bacteria. In the negative control, 50  $\mu$ L of 75  $\mu$ g/mL leaf extract of *R. serpentina* shows no ZOI (Figure 9A), but in presence of 50  $\mu$ L (1 mmol/L) silver nitrate solution, bacteria shows less ZOI (Figure 9A) in comparison with the AgNPs. At a low concentration of 25  $\mu$ g/mL of the AgNP, *E. coli* shows most significant effects with ZOI of (12.67  $\pm$  0.58) mm, whereas *B. subtilis* shows lesser effect with the zone size of (10.33  $\pm$  1.53) mm. The ZOI was increased with increasing concentration of synthesized AgNPs (Figure 9B). At the low concentration of ciprofloxacin (25  $\mu$ g/mL), *P. aeruginosa* shows more effective ZOI of (24.33  $\pm$  1.15) mm and *B. subtilis* shows less effective ZOI of (19.00  $\pm$  1.00) mm. With increasing concentration of ciprofloxacin, the ZOI was also increased (Figure 9B). The ZOI was not changed due to the combined effect of 50  $\mu$ L of 75  $\mu$ g/mL AgNPs and ciprofloxacin with respect to only ciprofloxacin (Figure 9A).

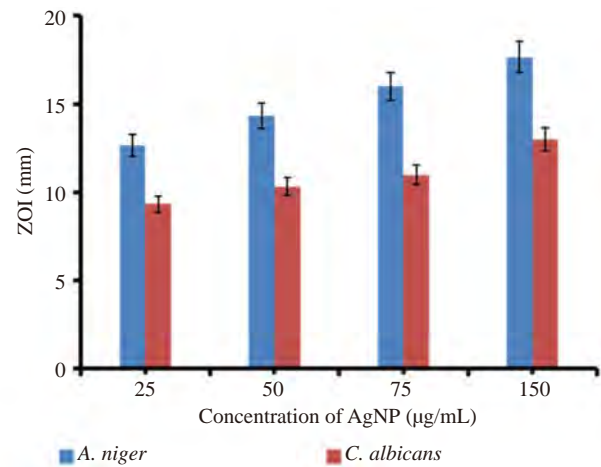
### 3.7. Fungicidal activity of the synthesized AgNP

The antifungal activity of the synthesized AgNP was carried out against *A. niger* and *C. albicans* at four different concentrations of the AgNP (25  $\mu$ g/mL, 50  $\mu$ g/mL, 75  $\mu$ g/mL and 150  $\mu$ g/mL). The *A. niger* shows more effective results than the *C. albicans*. At low concentration of AgNP (25  $\mu$ g/mL), *A. niger* shows the highest ZOI (12.67  $\pm$  1.15) mm, whereas *C. albicans* shows the lowest ZOI (9.33  $\pm$  0.58) mm. The effect of AgNP is increased in respect of the increasing of concentrations of AgNP (Figure 10). At concentration of 150  $\mu$ g/mL of AgNP, *A. niger* and *C. albicans* show (17.67  $\pm$  1.53) mm and (13.00  $\pm$  0.00) mm ZOI, respectively.



**Figure 9.** A: Antibacterial activity test result of synthesized AgNPs with *E. faecalis* (I), *B. subtilis* (II), *P. aeruginosa* (III), *E. coli* (IV) after 18 h of incubation at 37  $^{\circ}$ C; B: Graphical representation of ZOI for bacterial species against synthesized AgNPs (solid fill) and ciprofloxacin (light colour fill) at different concentration ( $\mu$ g/mL).

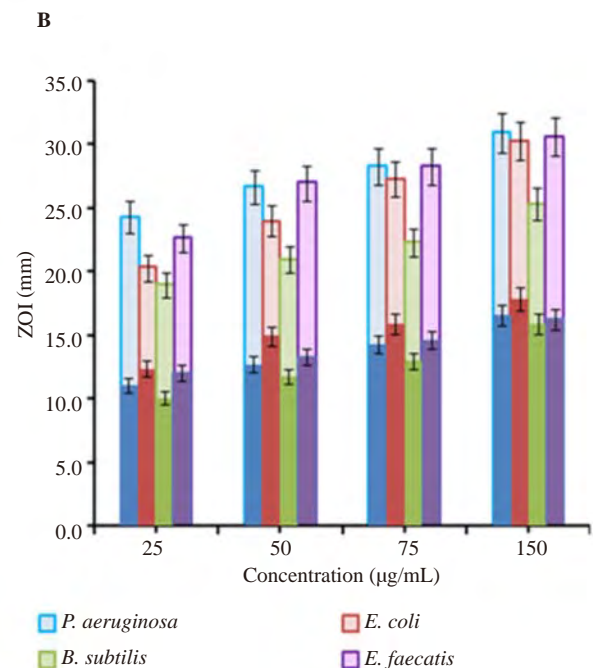
1: The concentration of 50  $\mu$ L of 1 mmol/L silver nitrate; 2: 50  $\mu$ L of 75  $\mu$ g/mL AgNPs; 3: 50  $\mu$ L of 75  $\mu$ g/mL leaf extract; 4: 50  $\mu$ L of 75  $\mu$ g/mL ciprofloxacin; 5: 50  $\mu$ L of 75  $\mu$ g/mL ciprofloxacin + 50  $\mu$ L of 75  $\mu$ g/mL AgNPs; Ciprofloxacin used as positive control.



**Figure 10.** Graphical representation of ZOI for fungal species against synthesized AgNPs at different concentration ( $\mu$ g/mL).

### 3.8. Larvicidal activity of the synthesized AgNP

The larvicidal activity of the synthesized AgNPs was performed against *Cx. quinquefasciatus* and represented in Figure 11 in dose dependent manner. From experimental value we concluded that the aqueous leaf extract of *R. serpentina* showed not more than (18.15  $\pm$  7.06)% mortality after 12 h incubation. On the other hand, pure silver nitrate solution of 1 mmol/L showed (10.74  $\pm$  11.13)% mortality after 12 h of incubation, while at 2.5  $\mu$ g/mL concentration of AgNPs it showed (62.1  $\pm$  4.77)% mortality after the same time of incubation. The experimental result showed that with increasing concentration of AgNPs, the percentage of mortality is also increased. The synthesized AgNPs showed maximum mortality (91.07  $\pm$  7.79)% at concentration 25  $\mu$ g/mL. The AgNPs synthesized from the leaf extract of *R. serpentina* showed significant efficiency against *Cx. quinquefasciatus*.



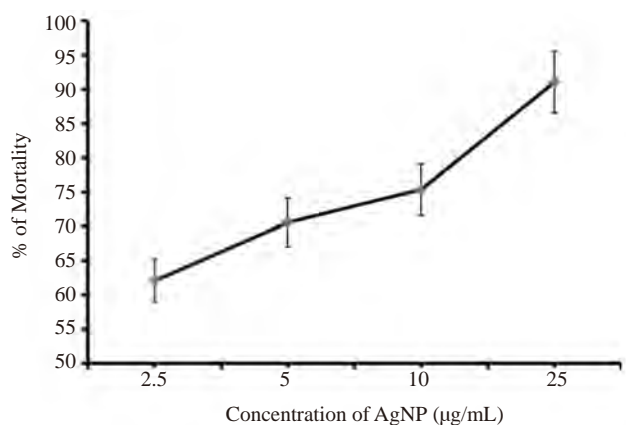


**Figure 11.** Percent of mortality of *Cx. quinquefasciatus* treated with different concentration of synthesized AgNPs.

### 3.9. Cytotoxicity assay of the AgNP

In cytotoxicity assay the synthesized AgNPs exhibit significant efficiency on HeLa, the cervical cancer cell line compared to MCF-7, the breast cancer cell line in dose dependent manner. The MCF-7 cell line shows the biphasic behaviour in presence of the AgNPs. At the concentration of 1.0 µg/mL of the AgNPs, MCF-7 shows 130.4 % rate of survival while HeLa shows 88.37%. At concentration of 2.5 µg/mL of the synthesized AgNPs, MCF-7 exhibits survival rate 77.67% whereas HeLa shows 65.28%. With the increase of the concentration of AgNPs the anticancer activity of the AgNPs also increases in both the cell lines (Figure 12).

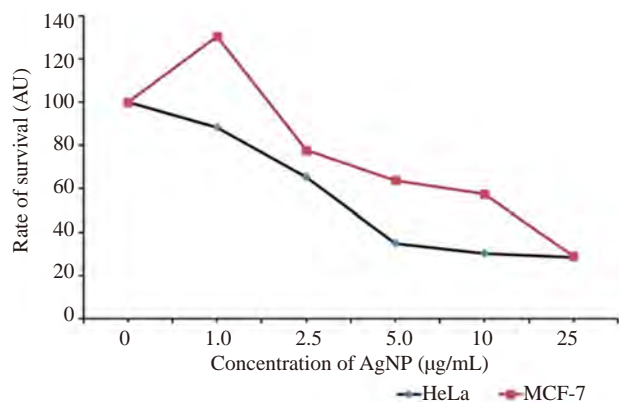


**Figure 12.** Graphical representation of rate of survival of HeLa and MCF-7 cell line treated with different concentration of synthesized AgNPs.

## 4. Discussion

The previous literature study shows that there are many examples of synthesized AgNPs from aqueous plant extract. The phytochemicals are rich in carbohydrate, tannin, alkaloids, flavonoids, steroids, for example 'Neem'. The phytochemicals are biodegradable, less toxic, eco-friendly and less costly. The presence of these groups is confirmed by the FTIR study. These groups are responsible for the reduction Ag(I) ion. The change of color during the synthesis of AgNPs from light yellow to yellowish brown confirms the synthesis of AgNPs from plant extract. The peaks of SPR due to the collective oscillation of the electron of the synthesized AgNPs from phytochemicals has similarity with the chemically synthesized AgNPs. The concentration of silver nitrate solution, plant extract, incubation time and temperature have significant effects on the synthesis of AgNPs. High as well as low concentration

of plant extract show aggregation of the synthesized AgNPs. This hydrothermal process requires thermal energy to synthesize the AgNPs from plant extract. At 90 °C there is no aggregation of the molecule. Low temperature and low incubation time show aggregation or no synthesis of the AgNPs from plant extracts. So this AgNPs synthesis process requires optimization of the synthesis condition.

AgNPs from *R. serpentina* leaf extract is synthesized in one step biological method which is eco-friendly, low cost, energy efficient and may be competitive alternative of the conventional physical or chemical methods. Different groups of the plant extract acting as both reducing and stabilizing agents are confirmed by FTIR analysis. The color changes during the synthesis of AgNPs and SPR at 427 nm confirm the synthesis of the AgNPs from the plant extract. We have synthesized spherical shaped AgNPs which is 7 to 10 nm in size and with crystalline nature. These AgNPs have similar antibacterial activity against both human pathogenic Gram-positive and Gram-negative bacteria. The synthesized AgNPs also show antifungal activity against human pathogenic fungus. This property of the synthesized AgNPs may be helpful in case of synthetic antibiotic resistant microorganism causing diseases. The AgNP produces free radicals[38]. The free radicals or the AgNP make bond with the cell membrane of the bacterial cell causing disruption of protein motive force[33] and damage the bacterial cell by forming pits on the surface. The mesosome cellular organelle of the bacterial cell which is present inside the cell membrane is responsible for the synthesis of major functional enzyme for cellular respiration, DNA replication and cell division, etc. The AgNP makes bonds with the mesosome cell organelle and decreases mesosomal function causing the inhibition of bacterial growth[7]. The synthesized AgNPs also have significant larvicidal activity against *Cx. quinquefasciatus*. It may provide a solution to control mosquito related diseases. Synthesized AgNPs have high cytotoxicity against cancer cell. The cytotoxicity study of the AgNPs shows more effect on HeLa, the cervical cancer cell line compared to MCF-7 the breast cancer cell line in a dose dependent manner. In conclusion, we may say that the effectiveness of synthesized AgNPs in biological application should be further studied as antimicrobial agent combining with antibiotics. The anticancer property of the nanoparticles might be further studied in other cancer cell lines.

### Conflict of interest statement

We declare that we have no conflict of interest.

### Acknowledgments

We would like to thank Mrs. Anindita Bhaumik for English editing.

### References

- [1] Metuku RP, Pabba S, Burra S, Hima Bindu SVSSSLN, K Gudikandula, Charya MAS. Biosynthesis of silver nanoparticles from *Schizophyllum radiatum* HE 863742.1: their characterization and antimicrobial activity. *3 Biotech* 2014; **4**(3): 227-34.
- [2] Sharma VK, Yngard RA, Lin Y. Silver nanoparticles: green synthesis and their antimicrobial activities. *Adv Colloid Interface Sci* 2009; **145**(1): 83-96.
- [3] Vijayaraghavan K, Nalini SP. Biotemplates in the green synthesis of silver nanoparticles. *Biotechnol J* 2010; **5**(10): 1098-110.
- [4] Zhou Y, Lin WS, Huang JL, Wang WT, Gao YX, Lin LQ, et al. Biosynthesis of gold nanoparticles by foliar broths: roles of biocompounds and other

- attributes of the extracts. *Nanoscale Res Lett* 2010; **5**(8): 1351-9.
- [5] Singh A, Jain D, Upadhyay MK, Khandelwal N, Verma HN. Green synthesis of silver nanoparticles using *Argemone mexicana* leaf extract and evaluation of their antimicrobial activities. *Dig J Nanomater Biostruct* 2010; **5**(2): 483-9.
- [6] Roy A, Khanra K, Mishra A, Bhattacharyya N. Highly cytotoxic (PA-1), less cytotoxic (A549) and antimicrobial activity of a green synthesized silver nanoparticle using *Mikania cordata* L. *Int J Adv Res* 2013; **1**(5): 193-8.
- [7] Gopinath K, Gowri S, Arumugam A. Phytosynthesis of silver nanoparticles using *Pterocarpus santalinus* leaf extract and their antibacterial properties. *J Nanostruct Chem* 2013; **3**(1): 68.
- [8] Kelly KL, Coronado E, Zhao LL, Schatz GC. The optical properties of metal nanoparticles: the influence of size, shape, and dielectric environment. *J Phys Chem B* 2003; **107**(3): 668-77.
- [9] Lewis BI, Lubin RI, January LE, Wild JB. Central nervous system and cardiovascular effects of *Rauwolfia serpentina*. *J Am Med Assoc* 1956; **160**(8): 622-8.
- [10] Bhatia BB. On the use of *Rauwolfia serpentina* in high blood pressure. *J Indian Med Assoc* 1942; **11**: 262-5.
- [11] Achor RW, Hanson NO, Gifford RW Jr. Hypertension treated with *Rauwolfia serpentina* (whole root) and with reserpine: controlled study disclosing occasional severe depression. *J Am Med Assoc* 1955; **159**(9): 841-5.
- [12] Kumari R, Rathi B, Rani A, Bhatnagar S. *Rauwolfia serpentina* L. Benth. ex Kurz.: phytochemical, pharmacological and therapeutic aspects. *Int J Pharm Sci Rev Res* 2013; **23**(2): 348-55.
- [13] Ahmed S, Saifullah, Ahmad M, Swami BL, Ikram S. Green synthesis of silver nanoparticles using *Azadirachta indica* aqueous leaf extract. *J Radiat Res Appl Sci* 2016; **9**(1): 1-7.
- [14] Khanra K, Panja S, Choudhuri I, Chakraborty A, Bhattacharyya N. Evaluation of antibacterial activity and cytotoxicity of green synthesized silver nanoparticles using *Scoparia dulcis*. *Nano Biomed Eng* 2015; **7**: 128-33.
- [15] Jain D, Daima HK, Kachhwaha S, Kothari SL. Synthesis of plant-mediated silver nanoparticles using papaya fruit extract and evaluation of their antimicrobial activities. *Dig J Nanomater Biostruct* 2009; **4**(3): 557-63.
- [16] El Kassas HY, Attia AA. Bactericidal application and cytotoxic activity of biosynthesized silver nanoparticles with an extract of the red seaweed *Pterocladia capillacea* on the HepG<sub>2</sub> cell line. *Asian Pac J Cancer Prev* 2014; **15**(3): 1299-306.
- [17] Von White G II, Kerscher P, Brown RM, Morella JD, McAllister W, Dean D, et al. Green synthesis of robust, biocompatible silver nanoparticles using garlic extract. *J Nanomater* 2012; **2012**: 730746.
- [18] Umashankari J, Inbakandan D, Ajithkumar TT, Balasubramanian T. Mangrove plant, *Rhizophora mucronata* (Lamk, 1804) mediated one pot green synthesis of silver nanoparticles and its antibacterial activity against aquatic pathogens. *Aquat Biosyst* 2012; **8**: 11.
- [19] Srinivasulu B, Prakasham RS, Jetty A, Srinivas S, Ellaiah P, Ramakrishna SV. Neomycin production with free and immobilized cells of *Streptomyces marinensis* in an airlift reactor. *Process Biochem* 2002; **38**(4): 593-8.
- [20] Yugandhar P, Savithamma N. Leaf assisted green synthesis of silver nanoparticles from *Syzygium alternifolium* (Wt.) Walp. characterization and antimicrobial studies. *Nano Biomed Eng* 2015; **7**(2): 29-37.
- [21] Arora R, Grewal A. Biogenic synthesis, characterization of silver nanoparticles from *Candelula officinalis* extract and evaluation of their antimicrobial activity. *Nano Biomed Eng* 2015; **7**(2): 47-51.
- [22] Malaka R, Hema JA, Muthukumarasamy NP, Sambandam A. Green synthesis of silver nanoparticles using *Cosmos sulphureus* and evaluation of their antimicrobial and antioxidant properties. *Nano Biomed Eng* 2015; **7**(4): 160-8.
- [23] Mondal NK, Chowdhury A, Dey U, Mukhopadhyaya P, Chatterjee S, Das K, et al. Green synthesis of silver nanoparticles and its application for mosquito control. *Asian Pac J Trop Dis* 2014; **4**(Suppl 1): S204-10.
- [24] Khadri H, Alzohairy M, Janardhan A, Kumar AP, Narasimha G. Green synthesis of silver nanoparticles with high fungicidal activity from olive seed extract. *Adv Nanopart* 2013; **2**: 241-6.
- [25] Kumar PS, Sudha S. Biosynthesis of silver nanoparticles from *Dictyota Bartayresiana* extract and their antifungal activity. *Nano Biomed Eng* 2013; **5**(2): 72-5.
- [26] Dhanasekaran D, Thangaraj R. Evaluation of larvicidal activity of biogenic nanoparticles against filariasis causing *Culex* mosquito vector. *Asian Pac J Trop Dis* 2013; **3**(3): 174-9.
- [27] Kamaraj C, Bagavan A, Elango G, Zahir AA, Rajakumar G, Marimuthu S, et al. Larvicidal activity of medicinal plant extracts against *Anopheles subpictus* & *Culex tritaeniorhynchus*. *Indian J Med Res* 2011; **134**: 101-6.
- [28] Tennyson S, Ravindran KJ, Arivoli S. Screening of twenty five plant extracts for larvicidal activity against *Culex quinquefasciatus* Say (Diptera: Culicidae). *Asian Pac J Trop Biomed* 2012; **2**(Suppl 2): S1130-4.
- [29] Khanra K, Panja S, Choudhuri I, Chakraborty A, Bhattacharyya N. Bactericidal and cytotoxic properties of silver nanoparticle synthesized from root extract of *Asparagus racemosus*. *Nano Biomed Eng* 2016; **8**(1): 39-46.
- [30] Khanra K, Panja S, Choudhuri I, Chakraborty A, Bhattacharyya N. Antimicrobial and cytotoxicity effect of silver nanoparticle synthesized by *Croton bonplandianum* Baill. leaves. *Nanomed J* 2016; **3**(1): 15-22.
- [31] Amin M, Anwar F, Janjua MR, Iqbal MA, Rashid U. Green synthesis of silver nanoparticles through reduction with *Solanum xanthocarpum* L. berry extract: characterization, antimicrobial and urease inhibitory activities against *Helicobacter pylori*. *Int J Mol Sci* 2012; **13**(8): 9923-41.
- [32] Li G, He D, Qian Y, Guan B, Gao S, Cui Y, et al. Fungus-mediated green synthesis of silver nanoparticles using *Aspergillus terreus*. *Int J Mol Sci* 2012; **13**(1): 466-76.
- [33] Netala VR, Kotakadi VS, Nagam V, Bobbu P, Ghosh SB, Tarte V. First report of biomimetic synthesis of silver nanoparticles using aqueous callus extract of *Centella asiatica* and their antimicrobial activity. *Appl Nanosci* 2015; **5**(7): 801-7.
- [34] Paulkumar K, Gnanajobitha G, Vanaja M, Rajeshkumar S, Malarkodi C, Pandian K, et al. Piper nigrum leaf and stem assisted green synthesis of silver nanoparticles and evaluation of its antibacterial activity against agricultural plant pathogens. *ScientificWorldJournal* 2014; **2014**: 1-9.
- [35] Kathiraven T, Sundaramanickam A, Shanmugam N, Balasubramanian T. Green synthesis of silver nanoparticles using marine algae *Caulerpa racemosa* and their antibacterial activity against some human pathogens. *Appl Nanosci* 2014; **5**(4): 499-504.
- [36] Paul JAJ, Selvi BK, Karmegam N. Biosynthesis of silver nanoparticles from *Premna serratifolia* L. leaf and its anticancer activity in CCl<sub>4</sub>-induced hepato-cancerous Swiss albino mice. *Appl Nanosci* 2015; **5**(8): 937-44.
- [37] Awwad AM, Salemb NM, Khrfan W, Ibrahim Q. FT-IR spectroscopy and X-ray diffraction characterization of biosynthesis silver/silver chloride nanoparticles. *Arab J Phys Chem* 2015; **2** (1): 14-9.
- [38] Shanmugam C, Sivasubramanian G, Parthasarathi B, Baskaran K, Balachander R, Parameswaran VR. Antimicrobial, free radical scavenging activities and catalytic oxidation of benzyl alcohol by nano-silver synthesized from the leaf extract of *Aristolochia indica* L.: a promenade towards sustainability. *Appl Nanosci* 2016; **6**: 711-23.